Wetting of Carbon Cathodes by Molten Electrolyte and Aluminium

Samuel Senanu[1*], Arne Petter Ratvik[1], Zhaohui Wang[1] and Tor Grande[2]
1. SINTEF Industry, Trondheim, Norway
2. Department of Material Science and Engineering, NTNU Norwegian University of Science and Technology, Trondheim, Norway
*Corresponding author: samuel.senanu@sintef.no

Keywords: Wetting, electrolyte, aluminium, carbon cathode, immersion, emersion

Abstract

The extent to which the carbon cathode is wetted by molten electrolyte or molten aluminium metal is important for understanding the cathode wear during aluminium electrolysis. The present paper reports on a laboratory study of the wettability of four different carbon materials using the immersion-emersion technique. The effect of polarization of the carbon cathode on the wettability was also included in the study. The measurements demonstrated that the carbon material is poorly wetted by the molten electrolyte or the metal. After polarization of the carbon in the cathodic direction the cathode became quickly wetted by the molten electrolyte. The presence of aluminium during the experiments resulted in enhanced wettability by the molten electrolyte. The carbon materials were analyzed by microscopy after the experiments and formation of Al_4C_3 was observed on the surfaces of the materials. The role of sodium in relation to enhanced wettability by molten electrolyte is discussed.

Introduction

Wetting is a key issue in many industrial processes, including aluminium electrolysis, due to the importance of solid-liquid interactions [1-3]. In aluminium electrowinning, wetting between the carbon anode and the molten electrolyte plays an important role in determining the size and coverage of CO_2 gas bubbles on the anode surface thereby influencing the ohmic resistance [4]. Wetting can also be assumed to affect the alumina dissolution process since a direct contact between the alumina grains and the bath is required after alumina hits and spreads on the surface of the bath [5]. Moreover, several of the processes that occur on the interface of the carbon cathode in industrial cells depends on the wetting properties between the carbon cathode and the two liquids present at the cathode, molten electrolyte, and liquid aluminium. Processes such as metal deposition, side ledge formation, melt penetration into the carbon lining, aluminium carbide formation and dissolution, sludge dissolution, etc. depend on the wetting between either the molten electrolyte or molten aluminium and the carbon cathode. Adequate wetting between molten aluminium and the cathode is also an important requirement for the design and operation of the so-called inert or drained cathodes [1, 6].

Laboratory investigations on the wettability of carbon by electrolyte melts have been discussed by Thonstad et al. [2]. In general, amorphous carbon tends to be better wetted by the electrolyte melt than graphite [2]. The wettability of the carbon cathode material by molten electrolyte is observed to improve after cathodic polarization [7-9]. Furthermore, the presence of metallic Al is observed to result in an improvement of the wettability between the molten electrolyte and carbon [10]. Different mechanisms including cathodic attraction [8], electrocapillary forces at bath/cathode interface [7], and metallic aluminium as a wetting agent have been mentioned as the reason for the improvement in wettability when the carbon material is cathodically polarized or liquid aluminium is present [8]. Liquid aluminium is observed not to wet the carbon cathode and this is attributed to the presence of an oxide layer surrounding the metal [10]. This is reflected in the reduced amount of Al_4C_3 formed when the metal is in contact with carbon [10]. Presence of the liquid cryolitic electrolyte is, however, proposed to aid the wettability as the carbide formation process is enhanced when the molten cryolite is present. The molten cryolite is proposed to work as a fluxing agent to dissolve the oxide layer [10, 11]. For the electrolysis cell, however, the presence of such an oxide layer surrounding the molten metal may be debatable due to the reducing conditions at the carbon cathode. Thus, the actual mechanism(s) behind improved wettability of carbon cathode by the molten electrolyte and aluminium needs further clarifications.

The present paper attempts to answer some of the questions regarding the mechanisms behind wettability. The investigations comprised the wettability of different types of carbon materials, anthracitic, graphitic, and graphitized carbon commonly used as cathodes in the aluminium industry, and a high-density graphite reference material. The study was based on the immersion-emersion technique previously reported by Martinez *et al*., modified to allow for polarization of the carbon materials during the experiments [1]. The carbon materials were examined by optical and electron microscopy before and after the wetting tests to investigate the infiltration of the melt into the carbon and the formation of Al_4C_3.

Experimental

A detailed description of the experimental set-up used for the wetting tests as well as the operation is described elsewhere [1]. Three industrial grade carbon cathode materials, anthracitic carbon (G0320), graphitic carbon (PB10), and graphitized carbon (EG) were used in the investigation. A fine-grained high-density graphite (G348) was included for reference. The densities of the different carbon samples were determined by measuring the geometric volume and mass. An Alicona Infinite Focus 3D optical profilometer was used to characterize the surface roughness of the pristine carbon materials while the permeability was measured using a Carbon R&D RDC - 145 air permeability apparatus. Data on the open porosity was obtained from the suppliers [12-14]. Cylindrical test specimens with 15 mm in diameter and 80 mm length were used. The samples were screwed onto a 250 mm long stainless-steel rod (6 mm dia.) suspended in a platinum wire to ensure that the lower surface of the sample was horizontal. Current cables were attached to the stainless-steel rod to enable polarisation during the measurements. The bath used in the experiments had a cryolite ratio (CR=mole NaF/mole AlF_3) of 2.2 and comprised of 80.75 wt% synthetic cryolite (≥ 97 %, Fluorsid), 4.5 wt% CaF_2 (97 %, Merck), 11.75 wt% AlF_3 (≥ 90,5 %, Noralf, Fluorsid) and 3 wt%

γ-alumina (≥99.5 %, Merck). Aluminium metal (99.9%, Alfa Aesar) was added as shots.

All the wetting measurements start by immersion of the carbon sample from an initial position of ca. 10 mm above the surface of melt to a specific lower position normally 10 mm from bottom of crucible at a rate of 0.2 mm/s. The sample was then kept at this position for a specific time, usually 30-60 s, before it was moved back to the initial position at the same rate of 0.2 mm/s. Thus, an immersion cycle in this study refers to the movement of sample from the initial position to the final position, while an emersion cycle refers to movement of sample from the final position back to the initial position. For tests involving both molten electrolyte and aluminium, the molten electrolyte and metal were kept at 35 mm and 25 mm, respectively. To investigate the wettability of the metal towards the carbon cathode, about 35 mm of the molten metal and 10 mm of molten electrolyte were used. Polarization of the samples in the cathodic direction was done for 30 seconds (electrolyte only) and 60 seconds (electrolyte and Al) applying a current density of ca. 1 A/cm^2 at the final position. Three samples each of the three traditional carbon cathode materials (anthracitic, graphitic, and graphitized) as well as two samples of the graphite material were measured for each test. Additionally, the measurement sequences were repeated three times for the different tests. The average data was used for the plots.

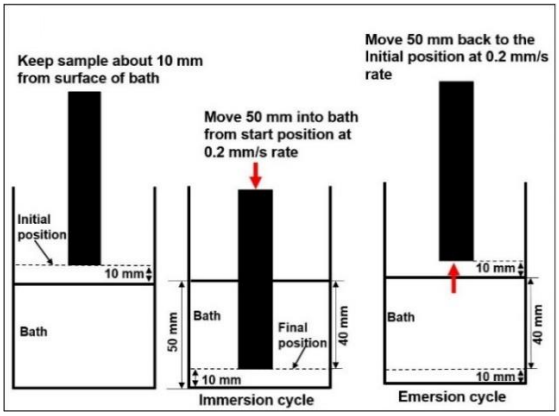

Figure 1: Illustration of the positions of the carbon sample relative to molten electrolyte during the immersion and emersion cycles in molten electrolyte.

The weight of the sample recorded during immersion/emersion were corrected for the buoyancy effect. The weight corrected for buoyance in the liquids, m_σ were calculated by

$$m_\sigma = (m_m - m_o) + f_b \times \Delta x \quad (1)$$

where m_m is the measured weight, m_o is the weight of sample in gas, f_b is the buoyancy correction factor and Δx is the difference between the actual position and the reference position of the sample. The reference position refers to the position where the sample came in physical contact with the liquid during immersion. The buoyancy correction factor, which represents the change in weight due to buoyancy per unit immersion depth, is given by

$$f_b = \pi r^2 \rho \quad (2)$$

where r (cm) is the radius of the circular cross-section of the sample while ρ (gcm^{-3}) is the density of the liquid in which the sample is being immersed.

Cross-sections of the cylindrical carbon cathode test samples from the wetting experiments were embedded in epoxy overnight and mechanically polished. The mechanically polished samples were then investigated using optical and scanning electron microscopy (SEM) as well as energy dispersive spectroscopy (EDS).

Results

Surface Roughness and Physical Properties of the Carbon Materials

Table 1 summarizes the physical properties, while Figure 2 displays the surface profile of all the four carbon materials measured by the optical profilometer.

Table 1: The physical properties of the four carbon samples used for the wetting tests [12-14].

Carbon Type (Trade name)	Density [g/cm^3]	Roughness [µm]	Air Permeability [nPm]	Open Porosity [%]
Anthracitic (G0320)	1.45±0.013	29.6	1.65±0.18	19
Graphitic (PB10)	1.63±0.004	18.2	1.12±0.12	20
Graphitized (EG)	1.74±0.005	8.4	0.49±0.01	13.5
Graphite (G348)	1.92	1.3	NA	8

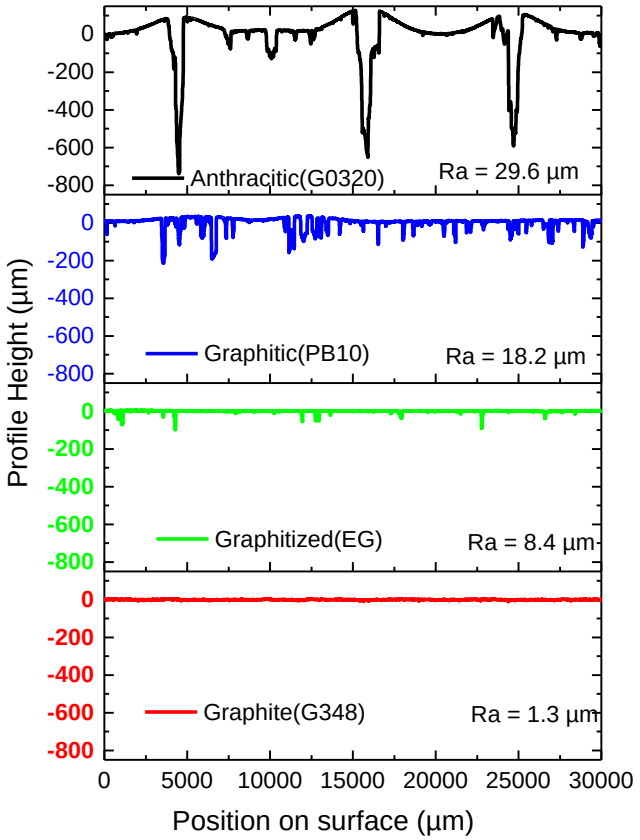

Figure 2: The surface profile of the four carbon materials showing the surface roughness values (Ra).

The surface roughness of the carbon materials can be ranged in the order anthracitic > graphitic > graphitized carbon > graphite (G348).

Large pores (mm range) in the anthracitic material are evident, while the size of the pores in the graphite materials (EG and G348) are significantly smaller, particularly in the case of the graphite G348 showing a very smooth surface profile.

Immersion-Emersion Data

A representative change in the weight of a cathode sample during an immersion/emersion cycle in the crucible containing molten electrolyte and aluminium is shown in Figure 3.

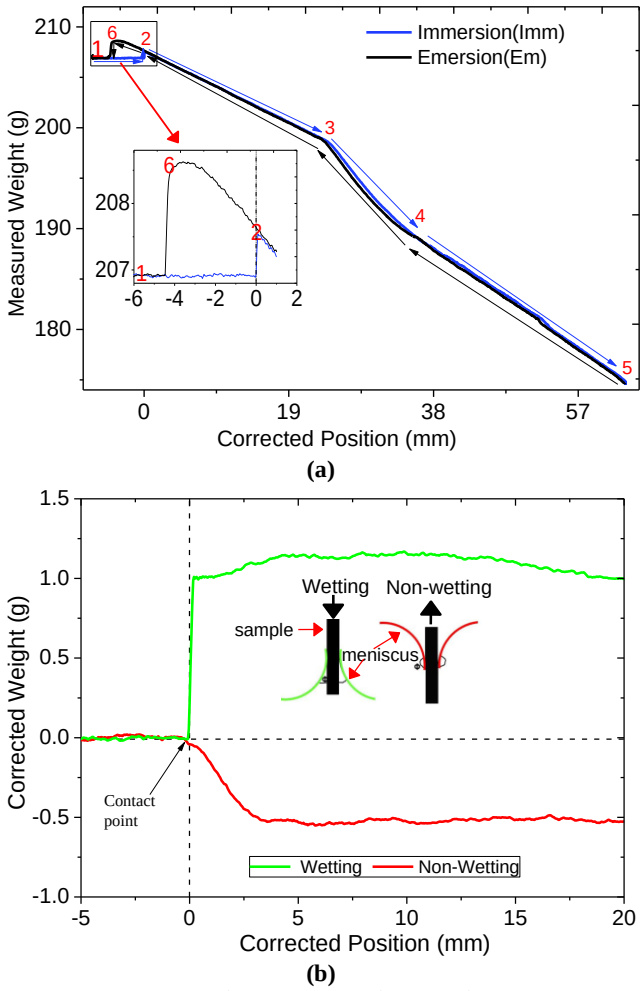

Figure 3: a) The weight of the sample as a function of its position relative to the molten electrolyte surface during the immersion/emersion cycle. Positions 1-6 are explained in the text. Insert: Magnified area of the initial part of immersion and final part of the emersion cycles. b) Changes in the weight of sample at the liquid surface position (contact point) illustrating a wetting and non-wetting situation. Insert: Meniscus formed by two liquids (a red non-wetting liquid and a green wetting liquid).

The changes in the weight is explained referring to the numbers in Figure 3a. The weight of the sample was constant between positions 1 and 2, where position 2 is the contact position. An instant change in weight was observed when the sample came in contact with the molten electrolyte due to formation of a meniscus at position 2. For samples wetted by the molten electrolyte, a weight increase was observed at position 2 (green curve in Figure 3b), while for samples not wetted, a weight decrease was observed at position 2 (red curve in Figure 3b). The weight of sample in both wetting and non-wetting cases continued to decrease as the sample was submerged into the molten electrolyte from position 2 to 3 due to the buoyancy effect. At position 3, the sample was in contact with the molten metal and a change in weight was recorded due to the formation of a metal meniscus around the sample. The sample penetrated into the metal at position 4. The average weight gradually decreased upon further immersion to position 5 due to buoyancy effect in the molten metal. The sample was then kept at this position for 30-60 s before the emersion cycle commences. The carbon samples were cathodically polarized by turning on a constant current with the sample at the final position (position 5) of the immersion cycle. During the emersion cycle, the weight of sample, represented by black curve in Figure 3a, follows roughly the same path as during the immersion cycle until the lower part of the sample reached the surface of the melt. At this position, the weight of the sample was observed to increase as it was lifted out of the liquid at position 2 before decreasing at position 6 in Figure 3a, close to the original weight prior to immersion. The time interval between position 2 and 6 was shorter for the non-wetting situation compared to the wetting situation.

The changes in weight at the contact position depends on the nature of the meniscus formed at the liquid surface as illustrated by the insert in Figure 3b. A liquid that wets the cylinder will form a concave meniscus upon contact during immersion and pull it downwards, resulting in a weight increase (green curve in Figure 3b). A liquid that does not wet the cylinder on the other hand will form a convex meniscus and push the sample upwards, resulting in a weight decrease (red curve in Figure 3b).

The average weight corrected for buoyancy during immersion/emersion in the molten electrolyte is shown for the four materials in Figure 4. In this case none of the carbon materials were polarized. The experiments revealed that the electrolyte did not wet the carbon materials during both immersion and emersion. Increasing the holding time at the final position during immersion did not change the wettability of the materials. The corrected weight is negative and relatively constant during the whole cycle, see Figure 4. The apparent noise in the weight signal is due to the deviation from the perfect cylindrical symmetry of the carbon cylinders due to surface roughness and open pores.

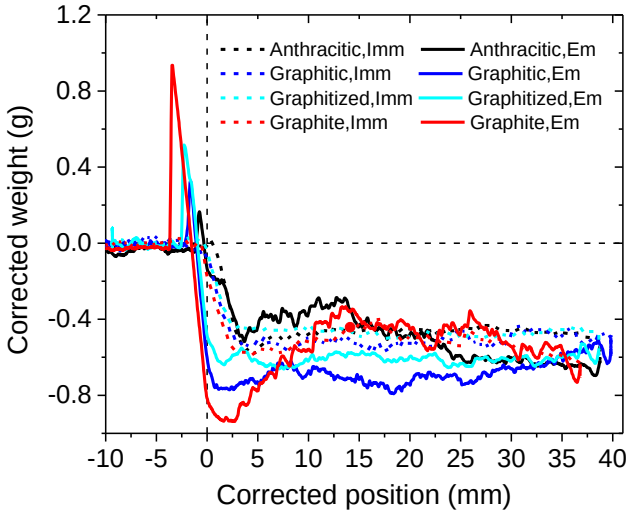

Figure 4: Average weight of the four materials corrected for the buoyancy effect during an immersion-emersion cycle with only electrolyte present in the crucible and no applied polarization of the materials.

The wetting experiments, shown in Figure 4, were repeated except that cathodic polarization of the carbon cylinders were applied for 30 s at the final immersion position. The buoyancy corrected data are shown in Figure 5a. The same non-wetting behavior as shown in Figure 4 is observed during immersion. However, during the period where the carbon cylinders became polarized, the corrected weight changes sign from negative to positive. The measured weight during this polarization period is shown in the Figure 5b, demonstrating the rapid weight increase as the voltage was turned on. The transition from a non-wetting to the wetting state is also clearly shown by the behavior during the emersion cycle. It was also observed that the final weight of the carbon cylinders was higher than the initial weight before the experiments. The increased weight after the experiments is explained by infiltration of molten electrolyte into the open pores. This gives additional evidence that molten electrolyte wets and infiltrates the carbon materials after polarization as no such weight increases were observed during the tests without polarization as in Figure 4.

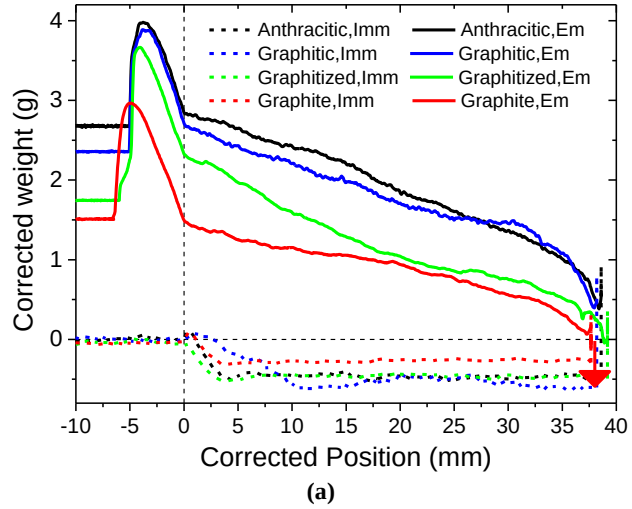

(a)

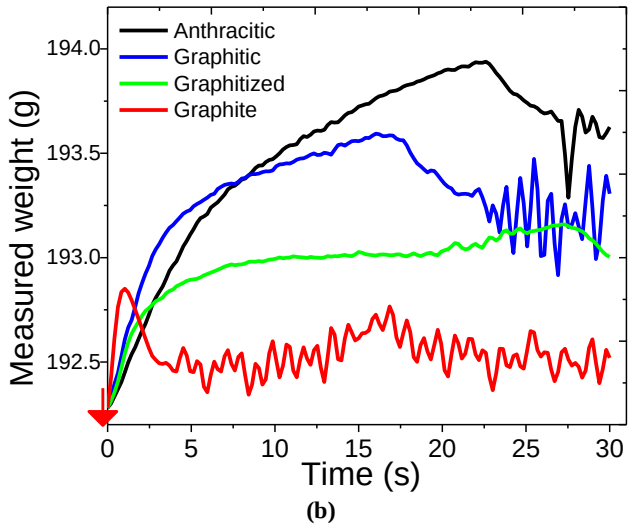

(b)

Figure 5: a) Average weight of the carbon samples corrected for the buoyancy effect during the immersion-emersion cycle with only molten electrolyte present. Red arrow indicates the position of the onset of polarization. b) Weight changes observed during polarization (30 s).

The immersion/emersion cycle were repeated after the experiments presented in Figure 5 but without the onset of polarization at the final immersion position. Data from successive cycles during a period of 24 hours demonstrated that most of the excess weight gained during the first complete cycle with polarization was gradually lost in the repeating cycles, shown in Figure 6. The weight signal also became less stable and the signature of wetting were less pronounced than in the first cycle.

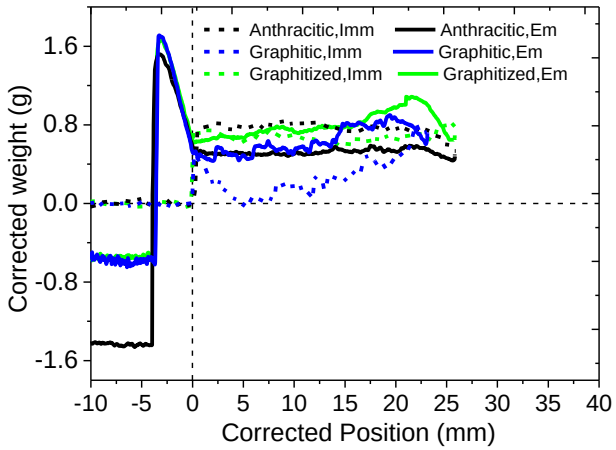

Figure 6: Average weight of the samples corrected for the buoyancy effect, 24 hours after the first cycle where polarization was applied for 30 s.

The wetting behavior of the carbon materials when the electrolyte is present together with molten aluminium are shown in Figure 7. The data show that all four carbon materials were wetted by the electrolyte when Al was present. All the data showed wetting prior to polarization, and upon polarization the wetting behavior did not change.

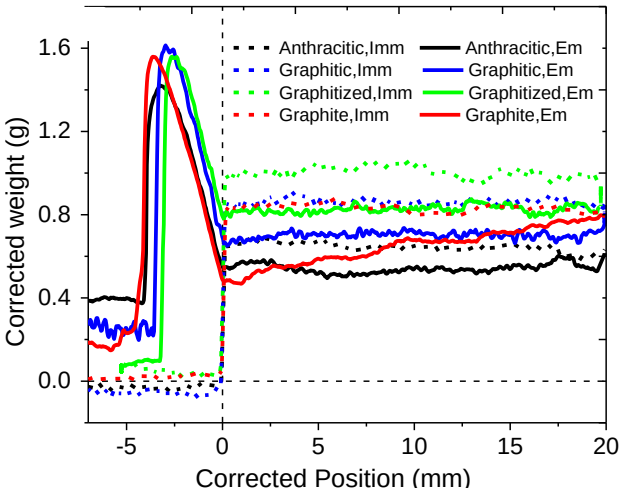

Figure 7: Average weight of the samples corrected for the buoyancy effect during an immersion-emersion cycle with molten electrolyte in contact with Al.

The wetting experiments performed in molten Al is shown in Figure 8. A positive corrected weight is observed only within the layer of electrolyte on top of the Al. Upon further immersion into the Al, only a negative corrected weight is obtained suggesting non-wettability. The data showed there is no wetting between the carbon cathode material and molten Al with or without cathodic polarization.

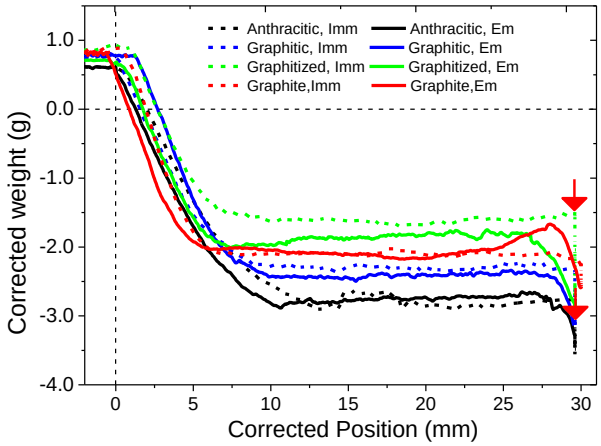

Figure 8: Average weight of the samples corrected for the buoyancy effect during an immersion-emersion cycles in molten Al for all four cathode samples with 60 s of cathodic polarization. Red voltage symbol indicates polarization position. Red arrows show start of cathodic polarization.

Characterization of the immersed carbon materials

SEM images of the non-wetted as well as the wetted carbon materials are displayed in Figure 9. The images demonstrate that molten electrolyte infiltrated the open pores of the carbon materials during wetting. The images show a higher amount of electrolyte within the anthracitic material as compared to the graphitic material. This difference may be due to the relatively larger open pores within the anthracitic material relative to the graphitic material. EDS mapping was used to confirm the presence of electrolyte within the carbon material.

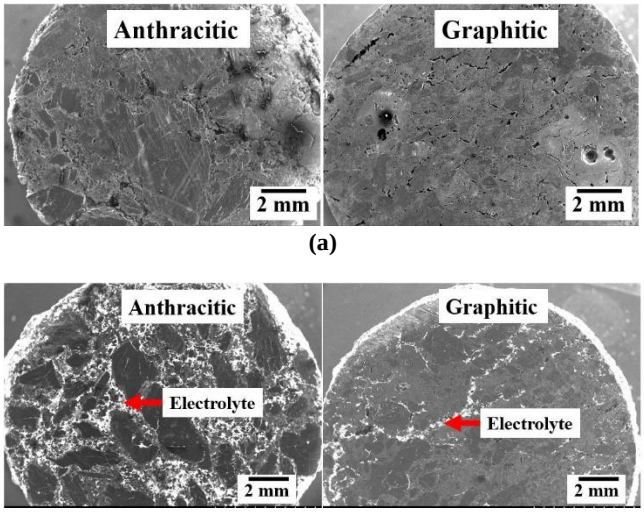

Figure 9. SEM images a) Anthracitic and graphitic carbon materials where no wetting has occurred. b) Anthracitic and graphitic carbon materials where wetting has occurred. White regions demonstrate solidified electrolyte within the porosities of the carbon materials.

The carbon materials used in the wetting tests conducted in molten electrolyte together with molten Al and polarized for a maximum of 300 s were analysed using SEM and EDS. SEM and EDS images of the interface between the carbon sample and the frozen electrolyte and aluminium metal is displayed in Figure 10.

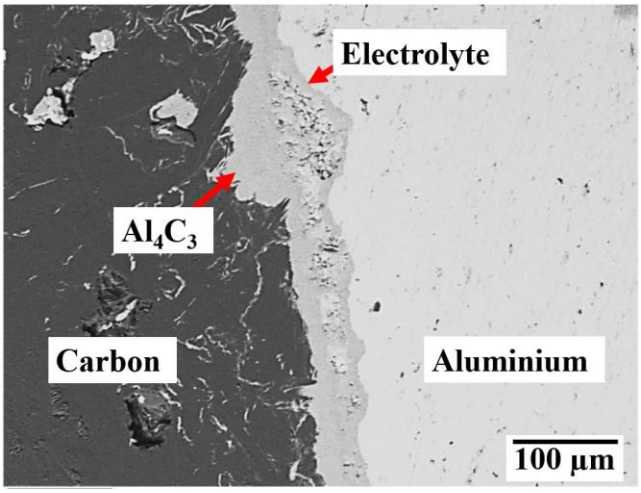

(a)

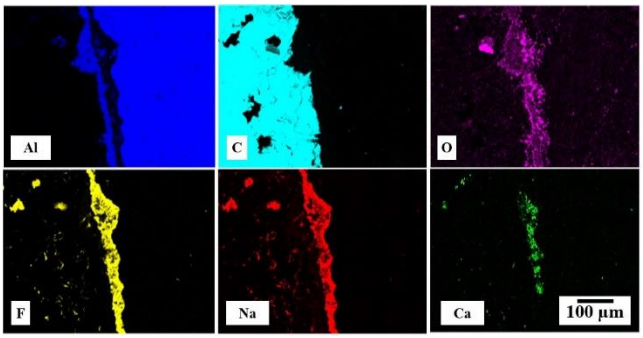

(b)

Figure 10. a) SEM image of the cut cross-section (red dashed line in) showing the carbon-Al interface. b) EDS element mapping of the carbon-Al interface from Figure 10a.

The SEM and EDS mapping shown in Figure 10 demonstrate the presence of two phases between Al and carbon. These two phases are observed as different shades of grey from the SEM images while the EDS mapping showed two distinct layers, one rich in F and Na and the other rich in Al. The layer rich in F and Na is proposed to be the electrolyte while the one rich in Al is proposed to correspond to Al_4C_3.

Images of the anthracitic carbon materials exposed to repeated immersion/emersion cycles after a 30 s cathodic polarization during the first cycle is shown in Figure 11. The image demonstrates that the amount of electrolyte that infiltrates the carbon material after wetting, as displayed in Figure 9b, was reduced after some time. This corresponds well with the data presented in Figure 6 where the weight of the samples after emersion declined with time.

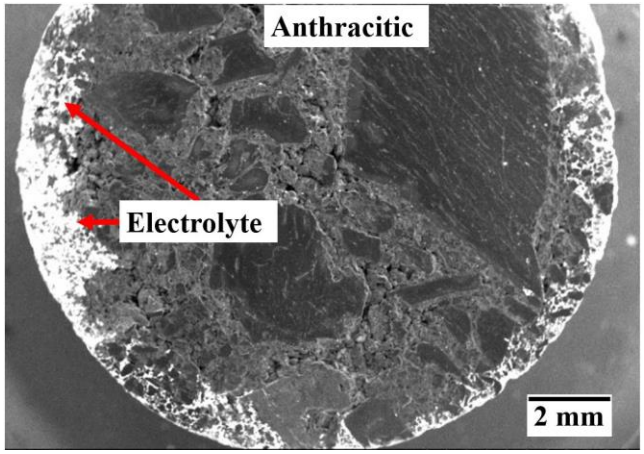

Figure 11. SEM images of anthracitic carbon samples after 24 hours of wetting tests in the molten electrolyte with 30 s of polarization.

Discussions

The wetting tests displayed in Figures 4 and 8 demonstrate that the carbon material is neither wetted by the molten electrolyte nor the liquid Al. However, upon cathodic polarization, as well as the introduction of metallic Al, the molten electrolyte is observed to wet the carbon materials as shown in Figures 5 and 7, respectively. It is proposed that the mechanisms behind the enhancement of wettability during cathodic polarization and during the introduction of metallic Al are related. We propose that this is due to an enhanced activity of Na, as described by Equation 1 to 3. The increased Na activity will result in intercalation of Na in the carbon material resulting in improved wettability and the consequent penetration of electrolyte into the porosity of the carbon material.

$$Na^+(diss) + e^- = Na\,(inC) \quad (1)$$

$$3NaF(diss) + Al(l) \rightleftharpoons 3Na(inAl) + AlF_3(diss) \quad (2)$$

$$Na(inAl) \rightleftharpoons Na\,(inC) \quad (3)$$

Infiltration of electrolyte into the open pores of the carbon materials was observed as an increase in weight, this is shown in the insert in Figure 5. It can be seen from these data that the infiltration occurred relatively fast suggesting that this is a surface related phenomenon as the time required for Na diffusion into the bulk of the carbon material is significantly longer [15, 16]. It is therefore proposed from the present results that the presence of Na on the cathode surface is sufficient and the necessary condition to initiate wetting and the consequent penetration of electrolyte into the porosity of carbon. It was generally observed that the highly amorphic carbon materials contained more electrolyte within the porosity compared to the other materials. Additionally, it can be seen from Figure 3, that the pores of the more amorphic anthracitic cathode sample were significantly larger than that of the graphitic samples. The larger pores will contribute to more bath entering the structure of the carbon material.

The wettability induced during cathodic polarization was observed to remain even after the voltage had been switched off as shown in Figure 6. It is, however, shown that during successive emersion/immersion cycles without cathodic polarization the amount of infiltrated electrolyte declined over time. The decrease in the excess weight as function of time after the experiments is attributed to reduced wettability. It is proposed that the decreasing wettability results from decreased Na activity after the voltage was switched off. Intercalation of Na into the carbon material is well documented to be reversed when the factors responsible for the insertion are removed [15, 17-19]. Switching off the current results in a reduction of the Na activity as the electrochemical Na production given by Equation 1 is terminated. Consequently, the driving force for bath penetration into the carbon material is reduced when the Na activity in the carbon material is reduced, i.e. the reversible nature of Na intercalation in carbon [15, 17, 18]. Consequently, once the presence of Na in the carbon material is diminished, the effects induced by its presence such as wettability is also reduced. Impaired wettability may then result in weakened attraction between the electrolyte and carbon thereby allowing gravity to drain the electrolyte out of the carbon materials. This is also evident from Figure 11 where most of the electrolyte within the carbon material is drained, leaving only the electrolyte close to the surface of the cylinder in contact with the bath. The remaining electrolyte explains why the sample apparently is still wetted by the electrolyte since the electrolyte on the cathode surface will be wetted by the bulk electrolyte during the immersion and emersion cycles.

The formation of Al_4C_3 on the cathode surface may also influence the wettability as the electrolyte is shown to wet the carbide, shown in Figure 10. Thus, if carbide is formed during the polarization stage, the carbide layer on the surface will be wetted by the electrolyte even when the voltage is switched off until no more carbide is left. However, for the present tests, the time for cathodic polarization was too short for any appreciable level of carbide to form. Furthermore, for the carbide to form, wetting would first have to be established between the carbon cathode and the electrolyte. Thus, even though the presence of Al_4C_3 may influence the wettability, it is not the primary cause of the observed wettability.

The results displayed in Figure 10 show that aluminium carbide formation does not necessarily occur by a direct contact between the metal and carbon cathode. Rather the presence of electrolyte between the carbide layer and the metal as shown in Figure 10 suggest that carbide formation may occur between the electrolyte and carbon in the presence of Na. Equation 4 shows that aluminium carbide can be formed between the electrolyte and carbon in the presence of Na intercalated in carbon. The NaF that is produced in addition to the Al_4C_3 from the reaction can be assumed as the reason for the F and Na rich layer displayed in the EDS image shown in Figure 10b.

$$4Na_3AlF_6(diss) + 12Na(in\,C) + 3C = Al_4C_3\,(s) + 24NaF(diss) \quad (4)$$

The fact that the carbon cathode is better wetted by the electrolyte than Al confirms that a film of electrolyte is present between the Al metal pad and the carbon cathode during electrolysis. This film of electrolyte, which is also observed on spent potlinings during autopsies, plays an important role in the cathode wear process as it influences the formation, dissolution and transport of Al_4C_3 from the cathode surface [20]. The formation of Al_4C_3 on the cathode surface in the presence of an electrolyte during electrolysis is strongly supported by reaction (4).

Conclusion

The present wetting tests of four different carbon materials have shown that carbon cathode is better wetted by the molten electrolyte than the molten Al under electrolysis conditions. Moreover, the present work confirmed the presence of a film of electrolyte between the Al metal pad and the carbon cathode. The mechanism behind enhanced wetting during cathodic polarization as well as introducing metallic Al is attributed to an enhanced Na activity at the cathode surface. Finally, the present findings also suggest that reaction 4 is important for the formation of Al_4C_3 during electrolysis.

Acknowledgement

Financial support from the Norwegian Research Council and Hydro, Alcoa, Elkem Carbon and Skamol through the project ‘‘CaRMa—Reactivity of Carbon and Refractory Materials Used in Metal Production Technology’’ is acknowledged (Grant No. 236665).

References

[1] Martinez AM, Paulsen O, Solheim A, Gudbrandsen H, Eick I (2016) Wetting Between Carbon and Cryolitic Melts. Part I: Theory and Equipment, in: Hyland M (Ed.) Light Metals 2015, Springer International Publishing, Cham, pp.665-670.

[2] Thonstad J, Fellner P, Haarberg GM, Hives J, Kvande H, Sterten A (2001) Aluminium Electrolysis: Fundamentals of the Hall-Héroult Process, Aluminium-Verlag Marketing and Kommunikation GmbH, Düsseldorf.

[3] Yuan Y, Lee TR (2013) Contact Angle and Wetting Properties, in: Bracco G, Holst B (Eds.) Surface Science Techniques, Springer, Berlin Heidelberg, pp.3-34.

[4] Martinez AM, Paulsen O, Solheim A, Gudbrandsen H, Eick I (2015) Wetting Between Carbon and Cryolitic Melts. Part I: Theory and Equipment *Light Metals* pp. 665-670.

[5] Thonstad J, Solheim A, Rolseth S, Skar O (1987) The Dissolution of Alumina in Cryolite Melts *Jom-J Min Met Mat S 39 (10)*, pp. A55-A55.

[6] Solheim A, Gudbrandsen H, Martinez AM, Einarsrud KE, Eick I (2016) Wetting Between Carbon and Cryolitic Melts. Part II: Effect of Bath Properties and Polarisation, in: Hyland M (Ed.) Light Metals 2015, Springer International Publishing, Cham, pp.671-676.

[7] Kvande H, Qiu ZX, Yao KS, Grjotheim K (1989) Penetration of Bath into the Cathode Lining of Alumina Reduction Cells *Light Metals*, pp. 161-167.

[8] Qiu Z-x, Wei Q-b, Yuo K-t (1983) Studies on Wettability of Carbon Electrodes in Aluminium Electrolysis (I) *Aluminium 59 (9)*, pp. 670-673.

[9] Utigard T, Toguri JM (1987) Radiographic Observation of the Hall-Heroult Electrolysis in Bench Scale Cells, 8. Internationale Leichtmetalltagung Leoben-Wien 1987, Aluminium-Verlag, Leoben-Wien pp.133-137.

[10] Doward RC (1973) Reaction between aluminium and graphite in the presence of cryolite *Met Trans B 4 (1)*, pp. 386-388.

[11] Sørlie M, Øye HA (2010) Cathodes in aluminium electrolysis, Aluminium-Verlag, Düsseldorf.

[12] Johansen JA (2018) Senior Specialist Carbon and Graphite Materials, Elkem Carbon AS Personal Communications, e-mail support.

[13] Ukrainsky Grafit Company (2019) Bottom Blocks. http://ukrgrafit.zp.ua/en/masspod. May, 2019 2019.

[14] (2019) Datasheet for G348 Graphite. http://schunk-tokai.pl/en/g348/. 19 November 2019.

[15] Ratvik AP, Støre A, Solheim A, Foosnaes T (2008) The effect of current density on cathode expansion during start-up *Light Metals* pp. 973-978.

[16] Wang ZH, Ratvik AP, Grande T, Selbach SM (2015) Diffusion of alkali metals in the first stage graphite intercalation compounds by vdW-DFT calculations *Rsc Advances 5 (21)*, pp. 15985-15992.

[17] Hop JG (2003) Sodium Expansion and Creep of Cathode Carbon, PhD thesis, Norwegian University of Science and Technology, Trondheim.

[18] Mikhalev Y, Øye HA (1996) Absorption of metallic sodium in carbon cathode materials *Carbon 34 (1)*, pp. 37-41.

[19] Thomas P, Billaud D (2002) Electrochemical insertion of sodium into hard carbons *Electrochim Acta 47 (20)*, pp. 3303-3307.

[20] Senanu S, Wang Z, Ratvik AP, Grande T (2020) Carbon Cathode Wear in Aluminium Electrolysis Cells *JOM 72 (1)*, pp. 210-217.